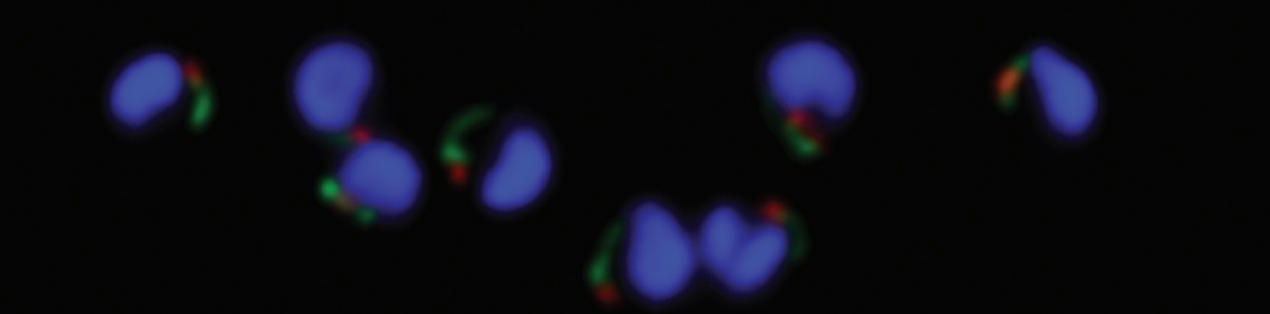


# molecular microbiology



**On the cover: Organelles in *Plasmodium***

**Integrating control by global regulators**

**Synchronized cultures**

**Ribosome-associated chaperones**



**Blackwell  
Publishing**

**Blackwell  
Synergy**



# Development of the endoplasmic reticulum, mitochondrion and apicoplast during the asexual life cycle of *Plasmodium falciparum*

Giel G. van Dooren,<sup>1†</sup> Matthias Marti,<sup>2‡</sup>  
Christopher J. Tonkin,<sup>1†‡</sup> Luciana M. Stimmer,<sup>1</sup>  
Alan F. Cowman<sup>2</sup> and Geoffrey I. McFadden<sup>1\*</sup>

<sup>1</sup>Plant Cell Biology Research Centre, School of Botany,  
University of Melbourne, Parkville, VIC 3010, Australia.

<sup>2</sup>The Walter and Eliza Hall Institute of Medical Research,  
Parkville 3050, Australia.

## Summary

*Plasmodium* parasites are unicellular eukaryotes that undergo a series of remarkable morphological transformations during the course of a multistage life cycle spanning two hosts (mosquito and human). Relatively little is known about the dynamics of cellular organelles throughout the course of these transformations. Here we describe the morphology of three organelles (endoplasmic reticulum, apicoplast and mitochondrion) through the human blood stages of the parasite life cycle using fluorescent reporter proteins fused to organelle targeting sequences. The endoplasmic reticulum begins as a simple crescent-shaped organelle that develops into a perinuclear ring with two small protrusions, followed by transformation into an extensive reticulated network as the parasite enlarges. Similarly, the apicoplast and the mitochondrion grow from single, small, discrete organelles into highly branched structures in later-stage parasites. These branched structures undergo an ordered fission – apicoplast followed by mitochondrion – to create multiple daughter organelles that are apparently linked as pairs for packaging into daughter cells. This is the first in-depth examination of intracellular organelles in live parasites during the asexual life cycle of this important human pathogen.

## Introduction

The malaria-causing parasite *Plasmodium falciparum*

undergoes a 48 h cycle of asexual replication and division in human erythrocytes. This asexual cycle causes all of the clinical symptoms of the disease, and commences when small, extracellular merozoites actively invade blood cells, by means of an actin-myosin motor (Cowman and Crabb, 2002; Morrisette and Sibley, 2002; Soldati and Meissner, 2004). Upon entry into the erythrocyte, ring-stage parasites begin to modify their host cell through export of remodelling factors and a series of variable antigens. One day into the two-day life cycle, parasites begin to ingest the abundant haemoglobin of their host erythrocyte by an endocytic process (Aikawa *et al.*, 1966). To avoid the toxic effects of haem, trophozoite-stage parasites polymerize this molecule within their food vacuole and use the remaining components for nutrients. After almost complete consumption of the erythrocyte, trophozoites undergo so-called schizogony, a series of nuclear divisions without subsequent cytokinesis to form multinucleated schizonts. Schizonts undergo cell division to form as many as 32 merozoites, which burst out of the remnant red blood cell and reinvest fresh erythrocytes.

Like all Apicomplexa, *P. falciparum* contains numerous intracellular organelles that function during this asexual cycle. Rhoptries and micronemes are secretory organelles that appear late in the cell cycle and release proteins crucial to the invasion process (Cowman and Crabb, 2002). Similarly, the food vacuole becomes evident at the transition between ring and subsequent trophozoite stages (Francis *et al.*, 1997). Certain other organelles are believed to persist in all stages of *P. falciparum*, and are not able to be formed *de novo*. For instance, all stages are assumed to contain endoplasmic reticulum (ER), a mitochondrion, an unusual unstacked Golgi and a plastid (known as the apicoplast) (McFadden *et al.*, 1996; Van Wye *et al.*, 1996; Bannister *et al.*, 2000). However, our knowledge of the behaviour of these organelles during the life cycle is limited to a handful of studies performed at the electron microscopy (EM) level. Two of these organelles, the apicoplast and the mitochondrion, are assuming increasing importance as drug targets as we learn more about their metabolism through genomics and biochemistry (Jomaa *et al.*, 1999; Srivastava *et al.*, 1999; Surolia and Surolia, 2001; Waller *et al.*, 2003).

Electron microscopy studies have identified the mitochondrion as a single crescent-shaped organelle in mero-

Accepted 22 April, 2005. \*For correspondence. E-mail gim@unimelb.edu.au; Tel. (+61) 3 8344 5054; Fax (+61) 3 9347 1071. †Present address: The Walter and Eliza Hall Institute of Medical Research, Parkville 3050, Australia. ‡Authors contributed equally to this work.

zoites that branches out in trophozoites, before segregating along with the nucleus into daughter merozoites (Aikawa, 1966; Slomianny and Prensier, 1986). Hopkins *et al.* (1999) created three-dimensional reconstructions of the apicoplast of *P. falciparum* from serial electron micrograph sections, focusing on merozoite, ring and trophozoite stages. They found the apicoplast to be a small, cylindrical structure, which lengthens during trophozoite stage (Hopkins *et al.*, 1999). Interestingly, EM studies revealed a close association between the apicoplast and mitochondrion at various stages during the intraerythrocytic cycle (Aikawa, 1966; Hopkins *et al.*, 1999). This mitochondrion/apicoplast association has been postulated to occur to allow transfer of metabolites between the two organelles (Hopkins *et al.*, 1999; Ralph *et al.*, 2004).

Despite its obvious value, EM is limited in its usefulness in *P. falciparum* for a number of reasons. First, membrane preservation in fixed parasites is generally poor, creating problems in identifying organelles in electron micrograph sections. Furthermore, serial sectioning is a labourious technique, making it difficult to analyse the large number of cells necessary to obtain an overall picture of an organism's organellar organisation. Imaging of live cells overcomes several difficulties associated with EM, and offers the potential of observing organellar morphology dynamically. The imaging of parasites expressing transgenic fluorescent proteins has been a significant addition to the tools used to study aspects of *P. falciparum* cell biology, and has been successfully employed to better understand protein targeting in parasites (Waller *et al.*, 2000; Kadakoppala *et al.*, 2001; Wickham *et al.*, 2001; Adisa *et al.*, 2003; Foth *et al.*, 2003; Klemba *et al.*, 2004; Marti *et al.*, 2004).

In this paper we have identified the minimum requirements for protein targeting and localization within the ER, which in turn has allowed us to examine ER morphology across the asexual life cycle. Furthermore, using two different selectable markers and a novel set of *P. falciparum* transfection vectors, which greatly simplify the process of making GFP fusion transfection constructs, we have created double transfectant lines expressing fluorescent proteins that target to the mitochondrion and apicoplast. Using nucleus number as a marker for the various stages of schizogony, we describe the complex morphological relationship between these two organelles during schizogony, and present a model for their segregation into daughter parasites.

## Results

### *Localization requirements for an ER protein and the morphology of the ER*

*PfBiP* contains a C-terminal SDEL motif, and it has been

postulated that this sequence mediates retention of BiP in the ER (Kumar *et al.*, 1991). To test this, we created a construct encoding a fusion protein consisting of the BiP signal sequence BiP(s), followed by the GFP reporter and the *PfBiP* SDEL motif appended to the C-terminus (Fig. 1B). We first confirmed expression of the fusion protein by Western analysis (Fig. 2A) and then its localization using immunofluorescence assays (IFA). As shown in Fig. 2B and C, the localization of GFP–SDEL largely overlaps with the endogenous BiP, demonstrating that the fusion protein is retained in the ER and that the reporter protein faithfully depicts the organelle structure.

With transgenic lines expressing GFP in the ER in hand, we set about characterizing the morphology of the ER in live cells. In early asexual-stage parasites, the ER has a simple morphology, consisting of a crescent shape that subsequently develops into a ring of fluorescence (Fig. 3A–C), presumably around the nuclear envelope (Fig. 2B and C), from which extensions emerge into the cytosol. We sometimes see 'horn'-like extensions emerging from the nuclear envelope (Fig. 3C arrows), which often extend around the food vacuole. In later stages, the ER appears to branch extensively through the cytosol, creating a complicated mesh-like network (Fig. 3D and E). After schizogony, maturing merozoites again show a crescent-like fluorescence pattern (Fig. 3F).

### *Generation of two-colour fluorescent parasites*

We generated two different MultiSite Gateway™ destination vectors, containing either hDHFR or blasticidin S as a selectable marker (Fig. 1A). This would allow for rapid selection of transgenic parasites maintaining both plasmids, and also sequential transfection of fusion proteins-of-interest into reference parasite lines already expressing a reporter protein. To test whether such a sequential double transfection was possible, we initially generated a parasite line expressing GFP fused to the leader peptide of the apicoplast protein ACP [ACP(l)], using the WR99210-resistant vector pCHDR-3/4 (see Fig. 1B) (Waller *et al.*, 2000). These cells show GFP with a typical apicoplast localization (Supplementary Fig. S1A–D) (Waller *et al.*, 2000). We next transfected this WR99210-resistant line (GFP in the apicoplast) with a plasmid conferring resistance to blasticidin S and localizing *DsRED* in the mitochondrion courtesy of the citrate synthase leader [CS(l)] (Tonkin *et al.*, 2004). This plasmid contains the BSD gene and utilizes the *PfCRT* promoter to drive the *DsRED* reporter (Fig. 1B). We were able to obtain double transfectants containing *DsRED* in the mitochondrion and GFP in the apicoplast (Supplementary Fig. S1). Expression of the *DsRED*, which was driven by the *PfCRT* promoter, was considerably weaker than the levels we typically observed when driven by promoters such as *PfHSP86* or

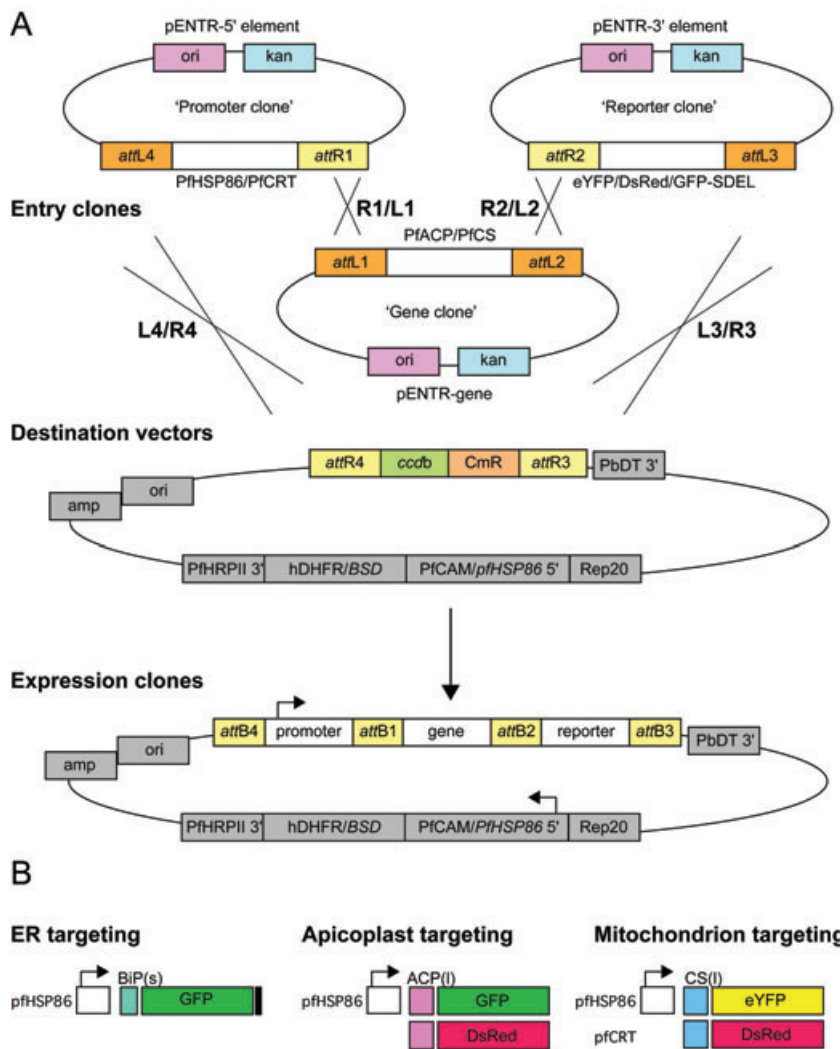


**Fig. 1.** Graphic representation of the cloning strategy using MultiSite Gateway™. **A.** The three types of entry clones created in this study containing either promoter elements ('Promoter clone'), the targeting sequence of a gene-of-interest ('Gene clone'), or the sequence encoding a fluorescent protein ('Reporter clone'). Destination vectors were created by ligating a 'cassette' containing *attL* recombination sites, a *ccdB* death gene and a chloramphenicol resistance marker (CmR) into an already established *P. falciparum* transfection vector (T. Voss and A. Cowman, unpubl.; O'Donnell *et al.*, 2002). To create an expression clone, one of each of the three entry clones (promoter, gene and reporter clone) plus a Destination vector are mixed together in the presence of a recombination enzyme mix that (after the appropriate selection regime) results in an expression clone containing promoter, gene and reporter all in a predictable order and orientation. ori, origin of replication; kan, kanamycin resistance gene; CmR, chloramphenicol resistance gene; *ccdB*, death gene which interferes with DNA gyrase and thus allows negative selection; *attR*1/2/3/4 and *attL*1/2/3/4, recombination sites. **B.** Targeting constructs made in this study. Five different expression clones – one being targeted to the ER, two to the apicoplast and another two to the mitochondrion. PfHSP86, *P. falciparum* Heat shock protein 86 gene; PfCRT, *P. falciparum* chloroquine resistance transporter gene; PfACP(I), Bipartite leader of *P. falciparum* acyl carrier protein gene; PfCS(I), Leader of *P. falciparum* citrate synthase gene; PfBiP(s), Signal peptide of *P. falciparum* BiP gene.

calmodulin (Waller *et al.*, 2000; Tonkin *et al.*, 2004; this study). This suggests that the PfCRT promoter will prove useful in expressing transgenes that are toxic to parasites when expressed in higher levels.

#### The morphology of the apicoplast during schizogony

No in-depth study has yet examined the morphology of the apicoplast or mitochondrion during schizogony and merozoite formation. To visualise these processes, we created a double transfectant line targeting eYFP to the mitochondrion and DsRED to the apicoplast. Both fusion proteins were generated by co-transfection of plasmids containing different selectable markers (Fig. 1). Western blot analysis demonstrated expression of the two fusion proteins (Fig. 4C). As a marker for schizogony we stained live cells with Hoechst 33258 nuclear dye and estimated the number of nuclei per cell after performing rotations on confocal sections of 100 cells. We categorized apicoplasts

into four morphological classes: rounded or ovoid apicoplasts, elongated apicoplasts, branched apicoplasts and divided apicoplasts [where these organelles are physically separated from each other; Fig. 4A(i–iv)]. We observed no absolute correlation between number of nuclei and apicoplast morphology, with cells containing a given number of nuclei having a range of possible apicoplast morphologies (Fig. 4A). Nevertheless, some clear patterns are apparent. Before the onset of schizogony (1 nucleus; Fig. 4A), apicoplasts are generally rounded in shape, although some elongated apicoplasts are also apparent. During early schizogony (2 and 3–5 nuclei), the apicoplast elongates, and ultimately begins to branch (6–10 nuclei). Late in schizogony (10–15 and >15 nuclei), the apicoplast undergoes a process of division.

#### The mitochondrion is a dynamic organelle

To investigate the morphology of the mitochondrion during



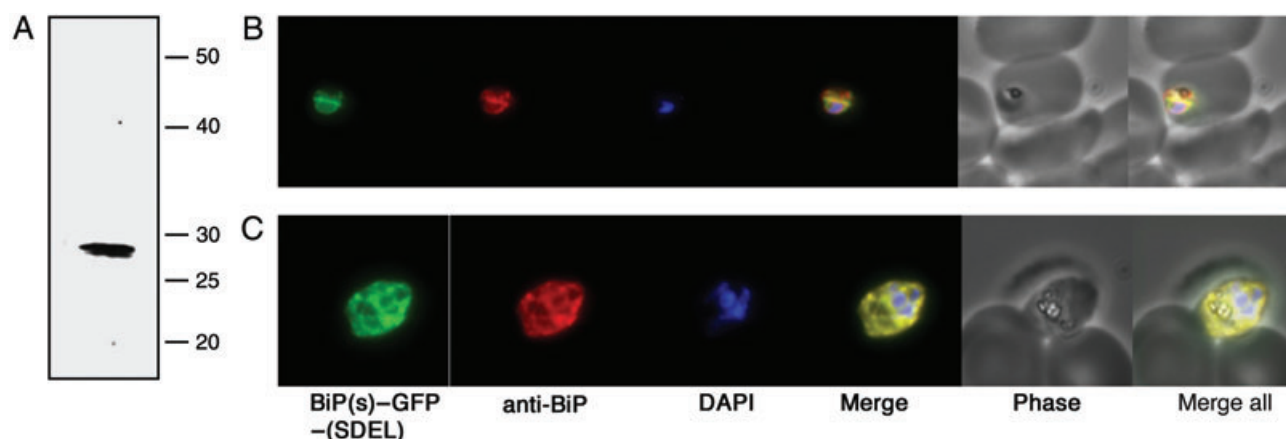


**Fig. 2.** BiP signal peptide fused to GFP and a C-terminal SDEL motif colocalizes with native BiP protein.

A. Western blot of BiP(s)-GFP-SDEL expressing cells showing a single band of predicted size for GFP-SDEL.

B, C. Immunofluorescent assays (IFA) of BiP(s)-GFP-SDEL expressing cells with GFP (green), anti-BiP (red) and nuclear staining with DAPI (blue). These images show that BiP(s)-GFP-SDEL colocalizes with native BiP, a known endoplasmic reticulum (ER) marker. In the cells shown here, the ER consists of a ring around the nucleus, plus some extensions into the cytosol. These results suggest that an SDEL motif is necessary and sufficient to retrieve *P. falciparum* proteins to the ER.

schizogony we examined eYFP fluorescence in the double transfectant line. We counted 100 double transfectants co-labelled with Hoechst 33258. The mitochondrion appears to be a dynamic organelle that undergoes numerous morphological changes during the intraerythrocytic cycle. Before schizogony, the mitochondrion may be elongated or branched (Fig. 4B). Elongated mitochondria typically have a cluster of more intense fluorescence at some point along the organelle [Fig. 4B(i)], and frequently appear to have contact points with the plasma membrane [Fig. 4B(ii) arrow; Fig. 5E right panel arrows]. Both branched and elongated mitochondria frequently contain looped regions, where the organelle appears to fuse back upon itself [Fig. 4B(ii and iii)]. We observed such fusions in 21% of the mitochondria examined in this analysis ( $n = 100$ ). After schizogony commences, branched mitochondria become the predominant form [Fig. 4B(iii)]. The mitochondrion appears as a single organelle for most of the asexual life cycle. Division apparently occurs very late in schizogony [Fig. 4B(iv)], with branched mitochondria remaining as the predominant form in cells with  $>15$  nuclei.

#### Association between the mitochondrion and apicoplast

In virtually all cells examined, there were apparent points of contact between the mitochondrion and apicoplast. In merozoite stages, the apicoplast and mitochondrion are single organelles that are closely apposed to each other (Fig. 5A and Supplementary Movie S1). Typically, the mitochondrion is slightly elongated with respect to the apicoplast. In rare cases we observe mitochondrial fluorescence that appears associated with the remnant food

vacuole after merozoite egress, but which is not associated with an apicoplast (Fig. 5A). In ring-stage cells, apposition between mitochondrion and apicoplast is maintained, with the mitochondrion forming a lengthened tubular organelle and the apicoplast remaining as a small, rounded organelle (Fig. 5B and C; Supplementary Movie S2). In early stages, a large proportion of the apicoplast surface is in contact with the mitochondrion. However, as the apicoplast begins to elongate in late trophozoite and early schizont stages, there is remarkably little apparent association between the organelles (Fig. 5D–F). The third panel in Fig. 5D, for example, shows stacked z-sections of the apicoplast and mitochondrion merged together. Single confocal optical sections reveal only a single contact point (Fig. 5D arrow), with the remainder of the two organelles clearly separate from each other. The early schizont cell in Fig. 5E contains an elongated apicoplast that has two contact points with the branched mitochondrion (arrows; Supplementary Movie S3). Similarly, Fig. 5F shows an early schizont containing an elongated apicoplast and branched mitochondrion. Two contact points are apparent between the organelles (arrows; Supplementary Movie S4). As schizogony proceeds, the number of contact points appears to increase (Fig. 4D). Cells containing elongated apicoplasts have, on average, 1.8 mitochondrial contact points ( $n = 27$ ), while cells with branched apicoplasts have, on average 4.1 contact points ( $n = 33$ ).

During the early stages of schizogony, apicoplast branches largely remain separate from mitochondrial branches, with a few contact points between them. Late in schizogony, we occasionally observe apicoplast branches aligning with mitochondrial branches (Fig. 6A

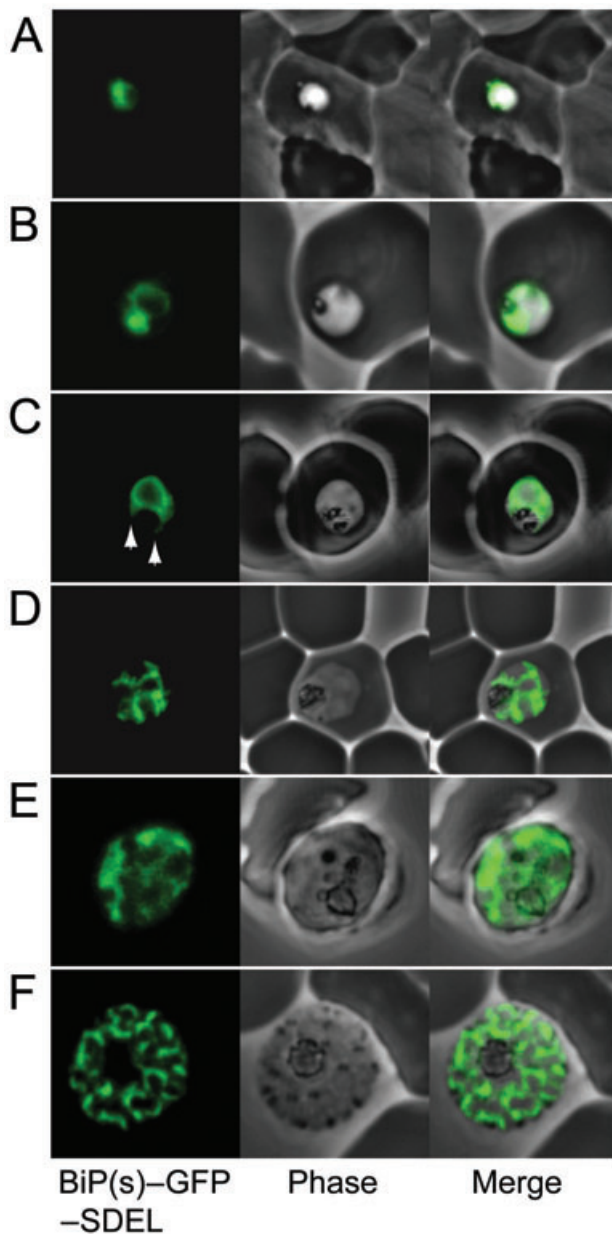


**Fig. 3.** Morphology of the ER during the asexual cycle of *P. falciparum*.  
 A. Shortly after invasion, the ER is a crescent-shaped organelle.  
 B, C. As the parasite begins to grow, the ER forms an entire ring around the nucleus (cf. Fig. 2B and C), which typically has two protruding horns coming from it (arrows in C).  
 D, E. Late-stage trophozoite or schizont-stage parasites where the ER becomes a complex, reticulated structure with numerous branches that extend through the cytosol.  
 F. Late schizont-stage parasite where the ER appears to fragment and form numerous crescent-shaped organelles. Presumably these represent the ER structure as seen in early ring stages (3A), with each daughter cell containing a crescent of ER fluorescence.

arrows; Supplementary Movie S5). In preliminary observations, we noticed that apicoplast division occurs reasonably late in schizogony, but always appears to occur before mitochondrial division. This held true in all cells we performed rotations for: we observed divided apicoplasts with branched mitochondria ( $n=12$ ) and divided mitochondria with divided apicoplasts ( $n=6$ ), but never divided mitochondria with branched or elongated apicoplasts. Remarkably, divided apicoplasts almost always associate with mitochondrial branches or with divided mitochondria. The top cell in Fig. 6B, for instance, shows divided apicoplasts with a branched mitochondrion. Each daughter apicoplast is clearly associated with a mitochondrial branch. In Fig. 6C the same holds true, although one of the divided apicoplasts appears separate from any mitochondrial branch (Fig. 6C arrow; Supplementary Movie S6). Observations of apicoplasts not associated with mitochondrial branches were rare, and it is not clear whether these apicoplasts correctly segregate into merozoites. In Fig. 6D the mitochondrion consists of a main branch that stretches out across the cell (Supplementary Movie S7). Emerging from this main branch are multiple smaller branches, many of which have a divided apicoplast associated with them. The divided apicoplasts and branched mitochondrion appear to be posterior to the nuclei.

Upon mitochondrial division, the situation seen in merozoites is re-established, with one apicoplast associated with one mitochondrion (Fig. 4D). Each apicoplast/mitochondrial pair typically localizes near to one nucleus of the schizont. Presumably, these each segregate into a single daughter merozoite. Figure 6E shows a late schizont where both apicoplast and mitochondrion have divided (Supplementary Movie S8). Most apicoplasts are clearly paired with a corresponding mitochondrion. Interestingly, one T-shaped mitochondrion appears associated with two apicoplasts (Fig. 6E arrow), suggesting that it may still be in the process of division.

## Discussion

### *Development of the parasite's endoplasmic reticulum*

The Hsp70-like protein BiP is a classical eukaryotic ER marker that regulates the specific folding and unfolding of proteins while also preventing protein misfolding and aggregation within the ER lumen. In other eukaryotes, BiP homologues are initially targeted to the ER via an N-terminal signal peptide, which is recognized by the signal recognition particle that docks with the Sec61 translocon thereby directing the nascent protein into the ER lumen (Couffin *et al.*, 1998). Retention of BiP, and other ER-resident proteins, in the ER is mediated by a C-terminal XDEL motif (where X can vary depending on species)

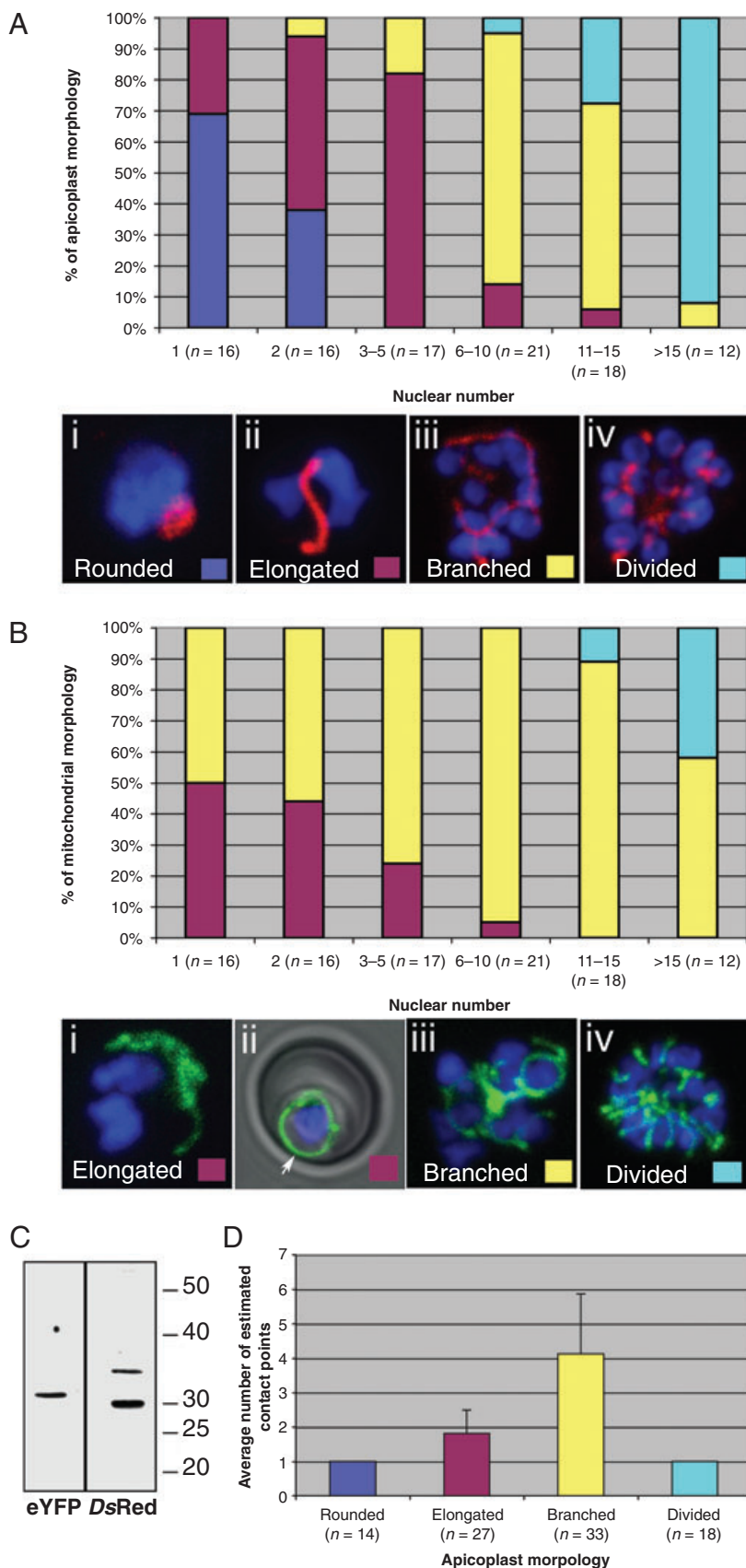


**Fig. 4.** Apicoplast and mitochondrial morphology and association during schizogony in *P. falciparum*. Live CS(l)YFP/ACP(l)DsRed double transfectant cells were co-labelled with the nuclear dye Hoechst 33258. One hundred cells were analysed to ascertain nuclear number and apicoplast and mitochondrial morphology. Nuclear number was determined by performing three-dimensional rotations of confocal sections.

A. Apicoplast morphology was categorized into four sorts: (i) rounded (ii) elongated (iii) branched and (iv) divided. Results indicated that at the onset of schizogony, the apicoplast is predominantly elongated in form. By the 6–10 nucleus stage, branched apicoplasts are the predominant form, with the majority of apicoplasts divided by the >15 nucleus stage.

B. Mitochondrial morphology was categorized as (i and ii) elongated (iii) branched and (iv) divided. The mitochondrion is a dynamic organelle, whose predominant form throughout the asexual cycle was branched. Mitochondrial division occurs very late in schizogony. The mitochondrion appears capable of fusion (ii and iii) and frequently associates with the plasma membrane (ii, arrow).

C. Western blot analysis on CS(l)-eYFP/ACP(l)DsRed double transfectant parasites. Left lane: Double transfectant line probed with anti-GFP antibody indicating the presence of a single band, corresponding to the expected size for CS(l)-eYFP with the CS(l) removed. Right lane: Double transfectant line probe with anti-DsRed antibody to detect ACP(l)-DsRed indicating the presence of two bands typical of an apicoplast targeted protein (van Dooren *et al.*, 2002).

D. Contact points between the apicoplast and mitochondrion are apparent at all times. In rounded apicoplasts, each associates with a mitochondrion. As the apicoplast matures, there are increasing numbers of contact points between the organelles. Elongated apicoplasts maintain on average 1.8 contact points with mitochondria, while branched apicoplasts have an average of 4.1 contact points. Upon apicoplast division, the number of contact points drops back to one, reflecting the fact that every divided apicoplast associates with either a mitochondrial branch or a divided mitochondrion. Error bars represent one standard deviation from the mean.



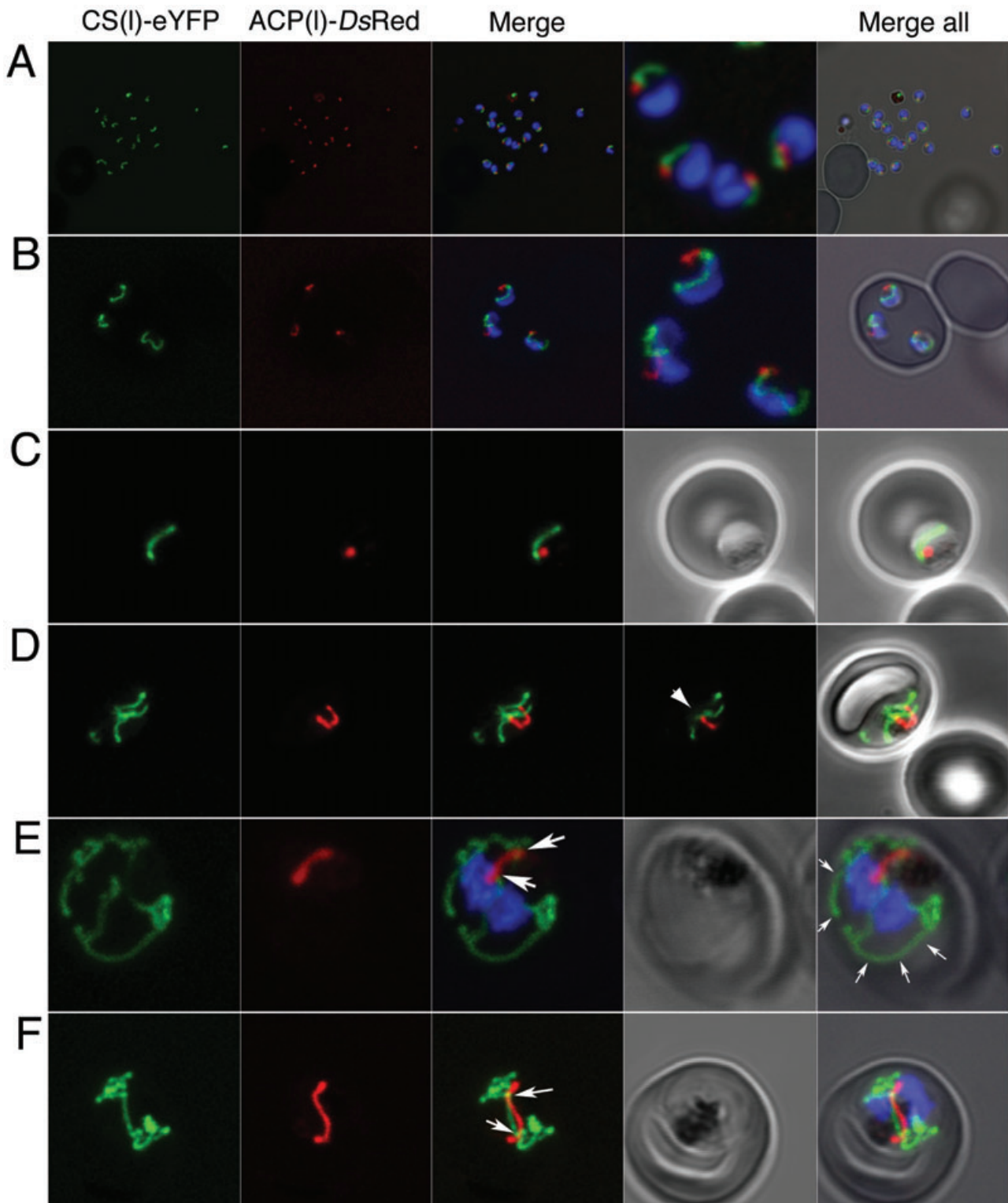


**Fig. 5.** The relationship between the apicoplast and the mitochondrion throughout the intraerythrocytic cycle. The apicoplast remains round- or ovoid-shaped from the merozoite stage (A) into ring (B) and trophozoite stages (C), whereas the mitochondrion appears as a rod-shaped organelle (A–C). By early schizogony, the mitochondrion is predominantly branched and the apicoplast elongated (D–F). The second panel from the right in D shows a single optical section of the merged image, showing a single point of contact between the two organelles (arrow). Such points of connection are also apparent in E (two points of contact; arrows) and F (two points of contact; arrows). The mitochondrion frequently associates with the plasma membrane (arrows in E, right panel). (See also Supplementary material, movies S1–S4, for 3D rotations.)



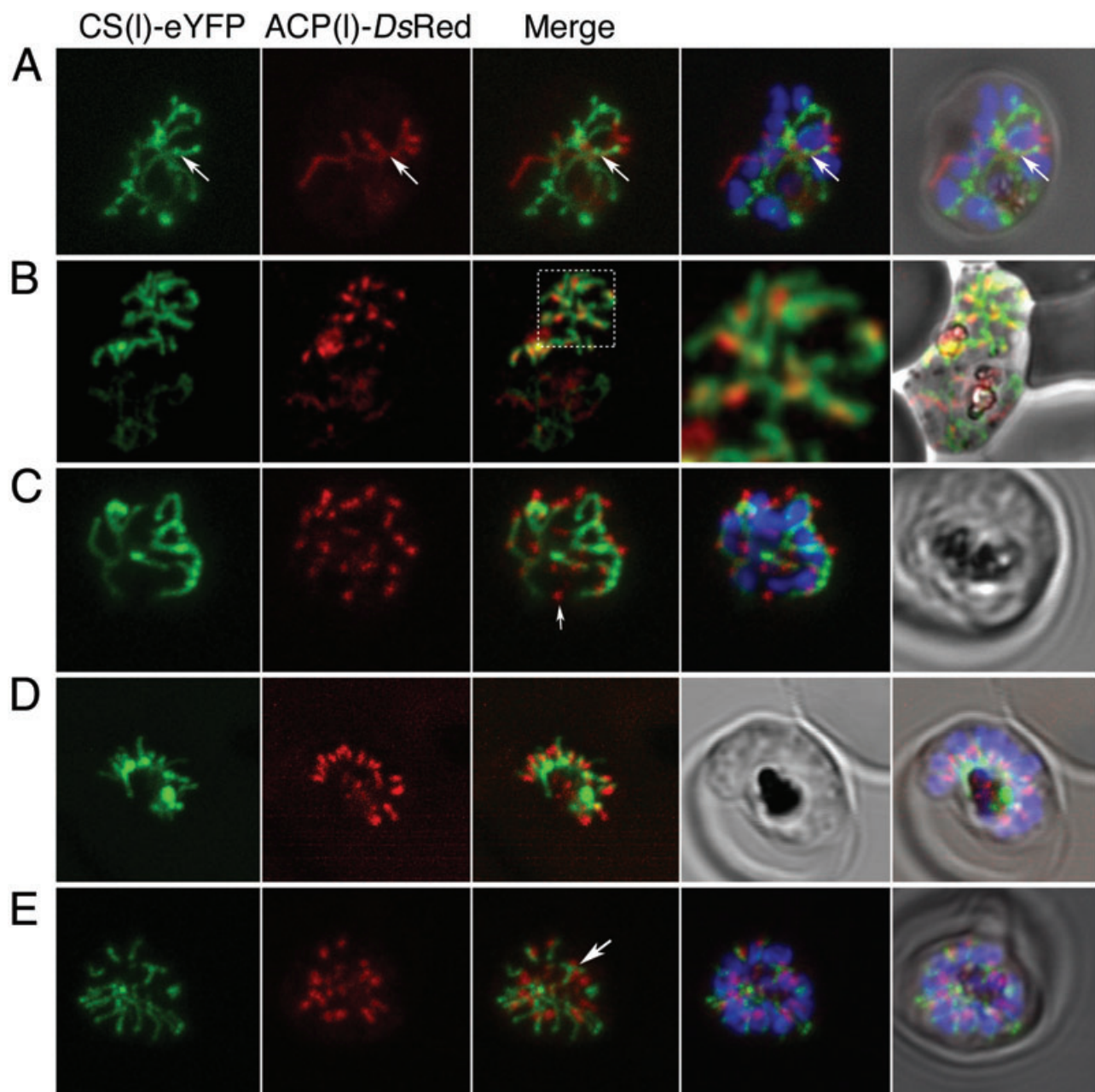


**Fig. 6.** Apicoplast division precedes mitochondrial division during schizogony. By mid-schizont stage, the majority of mitochondria are branched and the apicoplast also branches (A). Occasionally apicoplast branches appear to associate with mitochondrial branches (A arrows). The branched apicoplast always divides before the mitochondrion (B–D). Each segregated apicoplast closely associates with a branch of the mitochondrion (B–D). Fourth panel from the left in B shows a close-up of the boxed area in the third panel. Rarely, we observe apicoplasts not associated with a mitochondrial branch (arrow in C). The mitochondrion remains branched until apparently quite late in schizogony. Upon division, each mitochondrion associates with a divided apicoplast, and this organellar pair segregates into a single daughter merozoite (Figs 5A and 6E). Arrow in E shows a mitochondrion associated with two apicoplasts. Presumably, this mitochondrion is still in the process of division. (See also Supplementary material, movies S5–S8 for 3D rotations.)

(Munro and Pelham, 1987). Studies in yeast and other systems have shown that this XDEL motif is recognized by a protein known as ERD2 (endoplasmic reticulum retention domain receptor protein 2), which itself localizes to the *cis*-Golgi (Semenza *et al.*, 1990). ERD2 promotes retrograde transport of an XDEL-tailed protein back to the

ER. An ERD2 homologue is present in *P. falciparum* and it localizes to a perinuclear region (Elmendorf and Haldar, 1993). *PfBiP* contains a C-terminal SDEL motif that was expected to serve as an ER retention motif.

To test whether the *PfBiP* SDEL motif is sufficient for ER retention in *P. falciparum*, we created a construct with

three elements: the BiP signal peptide, GFP and an SDEL tail. This construct resulted in the reporter accumulating in the ER (Fig. 2B and C). By contrast, previous studies have demonstrated that a signal peptide–GFP fusion with no other targeting information results in secretion of the reporter protein (Waller *et al.*, 2000; Wickham *et al.*, 2001). This result is consistent with the hypothesis that a C-terminal SDEL signal is necessary and sufficient to retrieve soluble *Plasmodium* proteins from the Golgi into the ER to avoid secretion. *PfERC*, another *P. falciparum* ER-resident protein, contains an IDEL motif at the C-terminus (La Greca *et al.*, 1997), suggesting that, like other eukaryotes, the first amino acid of this motif can vary (Andres *et al.*, 1990). It is thus likely that XDEL motifs are recognized by *PfERD2* in the perinuclear *cis*-Golgi, from whence they are re-assorted back to the ER. Little is known about the morphology of the Golgi in *P. falciparum* and it will be useful to construct fluorescent reporter constructs fused to Golgi-resident proteins.

The establishment of a GFP parasite line targeting the ER allowed us to examine the morphology of this organelle across the asexual life cycle (Fig. 3). Beginning from short extensions from the nuclear envelope in early trophozoite parasites, the ER becomes a highly complex organelle by schizogony. It is likely that these changes in morphology reflects the increase in ER functions during the life cycle as the parasite becomes more metabolically active and grows to prepare for the mass formation of up to 32 daughter merozoites from a single schizont. The ER is involved in many processes, and in *P. falciparum* has been implicated in phospholipid biosynthesis (Baunaure *et al.*, 2004; Santiago *et al.*, 2004), GPI biosynthesis (Delorenzi *et al.*, 2002), calcium storage (Alleva and Kirk, 2001; Eckstein-Ludwig *et al.*, 2003), and trafficking of proteins to a range of destinations. The increase in activity of many of these processes during the asexual blood stages, and their cooperation with other cell compartments, possibly necessitates ER extensions throughout the cytosol. This is the first reported visualization of the ER throughout the erythrocyte life cycle of malaria parasites.

#### *Dynamics of the mitochondrion and apicoplast and their interaction during the cell cycle*

The functions of the mitochondrion and apicoplast of *P. falciparum* are a subject of considerable study, and these organelles are promising targets for a range of novel drugs (Waller *et al.*, 1998; 2003; Jomaa *et al.*, 1999; Srivastava *et al.*, 1999; Surolia and Surolia, 2001). Generating transgenic parasites with organelles labelled with different coloured reporter proteins has allowed us to study apicoplast and mitochondrial morphology and division. EM of merozoite and ring-stage cells has indicated that the apicoplast is a single, small, tubular structure that

lies in close proximity to the mitochondrion (Hopkins *et al.*, 1999), and our live cell images for this stage concur with these observations. The onset of schizogony coincides with some remarkable morphological changes in the apicoplast, which begins to elongate and branch and ultimately divide (Waller *et al.*, 2000; Waller and McFadden, 2005). The extensive branching of the *P. falciparum* apicoplast prior to fission into numerous daughter organelles is possibly an adaptation to schizogony. This contrasts with apicoplast division in *Toxoplasma gondii*, where binary fission of the organelle reflects the simple division of the mother cell into two daughters (Striepen *et al.*, 2000).

The mitochondrion in early stages is a narrow, tubular, often branched structure, as seen in previous live imaging of this organelle (Divo *et al.*, 1985; Slomianny and Prensier, 1986; Sato *et al.*, 2003; McMillan *et al.*, 2004). It was suggested that the mitochondrion begins branching during the transition from trophozoite to schizont (Divo *et al.*, 1985). Our data, however, indicate that mitochondria are frequently already branched at the onset of schizogony (Fig. 4B). It appears that the mitochondrion is a dynamic organelle in asexual stages, frequently appearing to fuse upon itself [Fig. 4B(ii and iii)], and often (but not always) seen in close association with the plasma membrane. Mitochondrial fusion has been observed in organisms such as budding yeast and land plants (Arimura *et al.*, 2004; Meeusen *et al.*, 2004), where it appears that mitochondrial morphology is regulated by a balance of mitochondrial fusion and fission. It is possible that such a balance between fusion and fission also exists in *P. falciparum*. The generation of fluorescent lines labelling the mitochondrion will allow fusion and fission events to be observed in live cells by time-lapse microscopy.

It is not clear why the mitochondrion associates with the plasma membrane in *P. falciparum*. One possibility is that the mitochondrion may serve as a conduit for plasma membrane phospholipids. In other organisms, the mitochondrion is a site for the biosynthesis of phosphatidylserine, and lipid exchange between the mitochondrion and the ER, plasma membrane and even plant chloroplasts have been observed (Jouhet *et al.*, 2004; Voelker, 2004). Unlike in these other organisms, however, phosphatidylserine biosynthesis appears not to occur in the mitochondrion of *P. falciparum* (Baunaure *et al.*, 2004), and it is not clear whether the organelle plays any role in lipid trafficking.

The resolution of confocal microscopy is not great enough to determine whether there is actual physical contact between the apicoplast and mitochondrion. Nevertheless, the close association between these two organelles at the various stages of the asexual cycle is striking, and EM shows close contact between these organelles (Aikawa, 1966; Hopkins *et al.*, 1999). Figure 7 summa-

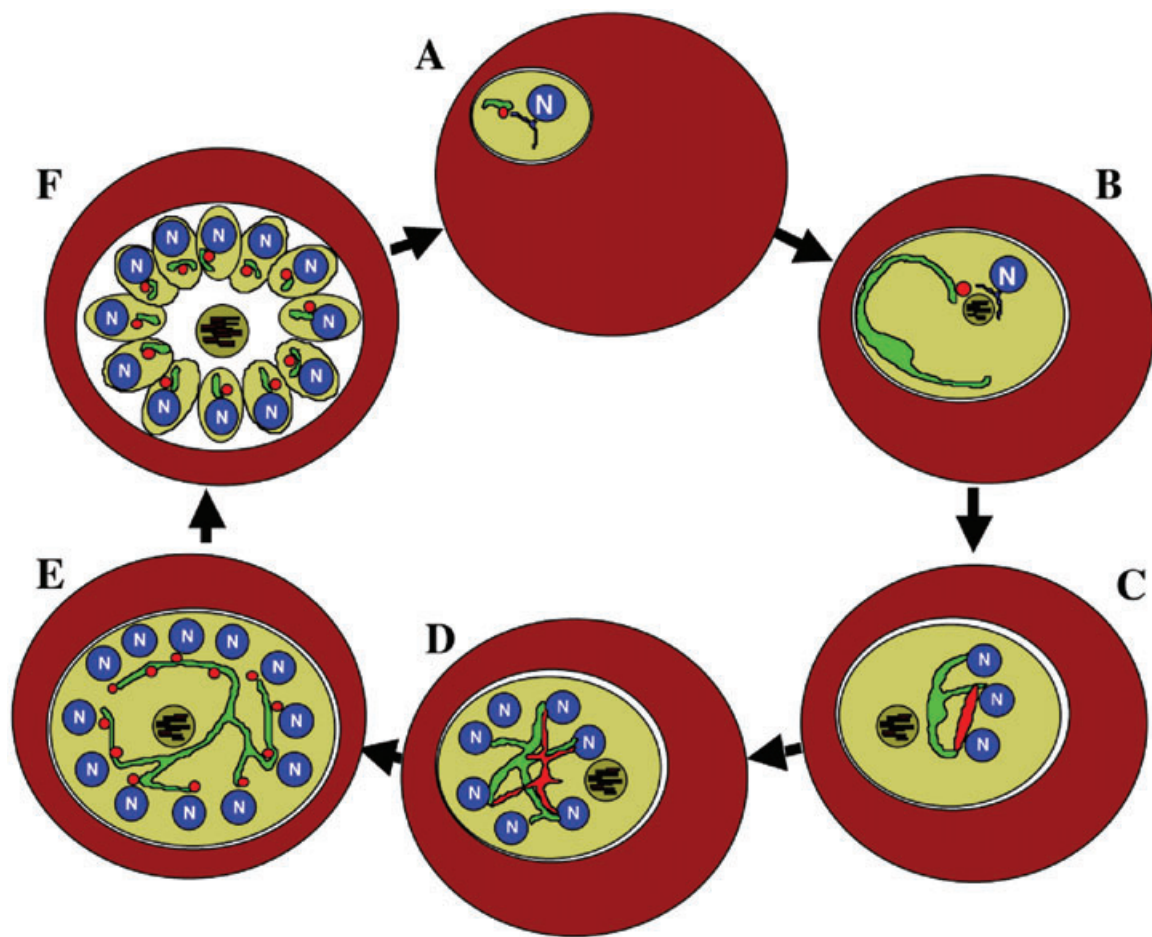


**Fig. 7.** A model for apicoplast/mitochondrial association across the intraerythrocytic life cycle of *P. falciparum*. At ring stage (A) the apicoplast and mitochondrion are in close association. The 'metabolic codependence' model suggests that this association exists to facilitate biosynthetic pathways that require enzymes found in both the apicoplast and mitochondrion (see text). In trophozoites (B), the mitochondrion begins to branch out through the cytosol, frequently associating with the plasma membrane. A contact point still exists between the two organelles, but the majority of the mitochondrial surface area is not in contact with apicoplast. The apicoplasts begin to elongate at the onset of schizogony (C) before branching out by mid-schizogony (D). The number of contact points between the apicoplast and mitochondrion increases during these stages. The apicoplast divides in late schizogony (E), with each divided apicoplast associated with the branched mitochondrion. Mitochondrial division appears to occur shortly before cell division, with each divided mitochondrion associating with a divided apicoplast. The 'co-segregation' model suggests that association of divided apicoplasts with the mitochondrion enables the subsequent segregation of these organelles as a connected pair into daughter merozoites (F).

rizes our current model for the apicoplast–mitochondrial interaction in *P. falciparum*. The two organelles are associated in ring and trophozoite stages (A and B). When the apicoplast begins to elongate at the onset of schizogony, contact points between the two organelles increases in number (C and D). The apicoplast always divides before the mitochondrion (E) and the two organelles segregate as a pair into daughter merozoites (F).

It has been suggested that association between the mitochondrion and apicoplast is required for metabolic interaction between these organelles (Aikawa, 1966; Hopkins *et al.*, 1999). For instance, it has been noted that haem biosynthetic pathway appears to be a composite of mitochondrial- and apicoplast-localized enzymatic steps (Varadharajan *et al.*, 2002; Ralph *et al.*, 2004; Sato *et al.*,

2004). This conjoined pathway perhaps necessitates an association of the two organelles (Ralph *et al.*, 2004). Although a metabolic bridge is an attractive rationalization of the apicoplast/mitochondrion link, a puzzling result from our cell cycle studies is the fact that the contact site does not expand during organelle and cell growth (Fig. 7). Indeed, the highly elongated or branched organelles of trophozoite/schizont stages, in which the apicoplast and mitochondrion are likely most active (Bozdech *et al.*, 2003), show only a few contact points. This prompted us to consider alternative or additional explanations for organelle contact.

Mitochondria and plastids cannot be derived *de novo* and must divide and be correctly segregated into daughter cells for organism survival. Upon division, each apicoplast



is associated with a mitochondrial branch (Fig. 7E). Upon mitochondrial division, each mitochondrion is subsequently paired with an apicoplast (Fig. 7F). We hypothesize that the association of the two organelles at this point allows for their correct segregation into daughter merozoites, ensuring that each merozoite contains a mitochondrion/apicoplast pair. Apicoplast division and segregation in the closely related parasite *Toxoplasma gondii* apparently involves tethering of the apicoplast to the centrioles and hitchhiking of the apicoplast on the mitotic machinery (Striepen *et al.*, 2000). Although *Plasmodium* parasites appear to lack obvious centrioles, they do contain spindle pole plaques that function in chromosomal division (Morrisette and Sibley, 2002), and the apicoplast could associate with these spindle poles. It is thus possible that the mitochondrion also hitches onto this division/segregation mechanism via the apicoplast. Association with the mitotic machinery would also provide a rationale for the observed branching of the apicoplast in *P. falciparum*. In *T. gondii*, the apicoplast elongates after centrosomal division, with either end of the apicoplast associated with a centrosome (Striepen *et al.*, 2000). In *P. falciparum*, spindle pole bodies presumably replicate numerous times before cell division. If the apicoplast remained associated with each of those bodies, a highly branched apicoplast would result. Although we often observe branched apicoplasts associating with all the nuclei in a cell [e.g. Fig. 4A(ii–iii)], we frequently see cells where not all nuclei are associated with an apicoplast branch (e.g. Fig. 6A), suggesting that apicoplast branching may not result from spindle pole body division. In such a scenario, divided apicoplasts would need to re-associate with spindle pole bodies before segregation for this theory to hold true. Once tools to identify spindle poles in *P. falciparum* become available it will be interesting to test these hypotheses with our double transfectants. We could further test our co-segregation model by disrupting processes of nuclear division or merogony to examine the effects that these have on segregation of the apicoplast and mitochondrion.

Testing the importance of the metabolic codependence scenario is not as simple. We might expect enzymes of the haem pathway to be concentrated at organellar contact points. Finding a method to disassociate the two organelles would allow us to examine whether the transfer of haem pathway intermediates is possible in the absence of a connection.

Our hypothesis for an apicoplast/mitochondrion link to enable proper organelle segregation is not mutually exclusive with the metabolic codependence scenario. Indeed, one may well have influenced the evolution of the other. For instance, the evolution of a physical contact site to ensure co-segregation may have been a spur for development of metabolic codependence. Conversely, the initial evolution of a metabolic codependence might have

required the origin of a physical contact point, and this association could then have been exploited as a means of keeping the organelles tethered during division and segregation.

Live cell imaging of *P. falciparum* provides a powerful way of examining the morphology, division and segregation of organelles such as the ER, apicoplast and mitochondrion. Based on observation, we have developed hypotheses on how these processes are mediated. It remains now to develop further techniques to test these hypotheses experimentally.

## Experimental procedures

### Destination vectors

To overcome many of the difficulties associated with creating *P. falciparum* transfection vectors (Tonkin *et al.*, 2004), we have utilized Invitrogen's Multisite Gateway™ technology to create a novel set of vectors. These vectors allow easy assembly of fluorescent protein constructs while allowing flexibility in promoter strength and timing, and permitting the use of different fluorescent proteins in conjunction with different targeting elements (Fig. 1). The Gateway MultiSite™ system involves the recombination of three so-called ENTR vectors, which we have designed to contain three separate elements of the expression cassette, with a so-called Destination vector, which we have engineered to encode *P. falciparum*-specific selectable markers. To enable creation of double transfectants, and for flexibility in choice of selectable marker, we created two destination vectors: one encoding human DHFR (hDHFR), which mediates resistance to WR99210 (Fidock and Wellem, 1997), the second encoding blasticidin-S deaminase (BSD), which creates resistance to the drug blasticidin-S. The destination vectors are modifications of the transfection vector pHBcam (A kind gift from T. Voss; T. Voss and A. Cowman unpubl.), which is itself a modification of pHHMC\*/3R0.5 (O'Donnell *et al.*, 2002). This plasmid contains two expression cassettes separated by a 0.5 kb rep20 element to improve episome segregation at mitosis (O'Donnell *et al.*, 2002). In line with the nomenclature we have previously described for Gateway plasmids created for *P. falciparum* (Tonkin *et al.*, 2004), we named the vector containing hDHFR pCHDR-3/4 (Calmodulin 5' driving human DHFR with rep20 in a head-to-tail (-) orientation with the attR3/R4 cassette). Similarly, the blasticidin S-resistant destination clone was named pHBIR-3/4 for HSP86 5' driving blasticidin S deaminase in a head-to-tail orientation (-) with the attR3/R4 cassette. Both destination vectors were made by ligating the Gateway attR4/R3 cassette into pHBcam. pHBcam contains expression cassettes for both BSD and a variant form of hDHFR. To create pCHDR-3/4, the attR3/R4 cassette was amplified from the commercially available plasmid pDEST™R4R3 using the primers GGGGTACCA GCTATGACCATGATTACGCCAAGCTATC (*KpnI* site underlined) and CCTCGAGACGTTGTAAAACGACGGCCAGTGA ATTATC (*XhoI* underlined) and then ligated into the *KpnI/XhoI* sites of pHH\_VP. pHBIR-3/4 was created by amplifying the attR3/R4 cassette using the primers GGAAGATCTGTACC GATCTTTCATATATATA (*BglII* underlined) and CAGTAAGC

TTAGCCCTCCACACATAACC (*Hind*III underlined) and ligating the amplification fragment into the *Bgl*II/*Hind*III sites of pHBcam. Both ligation reactions were transformed into CcdB-resistant DB3.1 *E. coli* (Invitrogen) and verified by sequencing (Fig. 1).

### pENTR vectors

The Gateway MultiSite™ system enables the recombination of three elements from pENTR vectors that results in them being placed in a specific order and orientation within the resulting destination vector. We designed the three pENTR vector elements to produce, after recombination, an expression cassette consisting of a promoter element, followed by a gene of interest (or part thereof) and a fluorescent reporter protein-encoding gene, with the terminator for the cassette encoded on the destination vector (Fig. 1A). The promoters we use in this study are the PfHSP86 5' region, known to drive high levels of transcription (Crabb *et al.*, 1997), and the PfCRT 5' region, which drives lower level expression of the chloroquine resistance membrane transporter (CRT). Our genes-of-interest included the leader sequence of citrate synthase (known to target the mitochondrion; Tonkin *et al.*, 2004), the full, bipartite leader sequence of acyl-carrier protein (known to target the apicoplast; Waller *et al.*, 2000) and the signal peptide region of the ER protein BiP. We utilized four separate fluorescent reporter proteins: enhanced YFP (eYFP), a monomeric form of DsRed (Campbell *et al.*, 2002), GFP (GFPmut2), and GFP modified to contain a SDEL sequence at its C-terminus (Fig. 1B), but our vector system enables the use of virtually any reporter protein or epitope tag.

The *P. falciparum*-specific promoter sequences were cloned into the commercially available pDONRP4-P1R vector (Invitrogen). The promoter sequences were amplified from genomic DNA, with the PfHSP86 5' region amplified using primers GGGGACAACCTTTGTATAGAAAAGTTGTCGT CGACGGAAAGGGGCCATTGGATATATA (*att*B4 underlined) and GGGGACTGCTTTTTTGTACAACTTGCAGATCTTTTA TTCGAAATGTGGGAAG (*att*B1 site underlined), and PfCRT 5' amplified using the primers GGGGACAACCTTTGTATA GAAAAGTTGTCGTCTGACTAGTAGTTGAGTGATTCTATATA CATATAC (*att*B4 site underlined) and GGGGACTGCTTTTTT GTACAACTTGCAGATCTGTTATATGTAAGAAATTAATAA AACAAAATAATAATGAATG (*att*B1 underlined). Each PCR product was mixed with pDONRP4-P1R in equimolar amounts in the presence of BP clonase as per manufacturer's instruction. Each BP reaction was transformed into CcdB-sensitive TOP10 *E. coli* and selected for kanamycin resistance. The resulting plasmids were named PfHSP86 5'-pENTR4/1 and PfCRT 5'-pENTR4/1 (Fig. 1).

GFP was amplified from the pHGB vector (Tonkin *et al.*, 2004) with primers GGGGACAGCTTTCTTGACAAAGTG GCACCTAGGAGTAAAGGAGAAGAACTTTCACTGGAG (*att*B2 underlined) and GGGGACCACTTTGTACAAGAAAGCT GGGTCCTGCAGTCTGGATTATTTGTATAGTTTCATC (*att*B3 underlined), whereas GFP-SDEL was amplified in a two-step process with the same *att*B2-containing primer as for GFP and TTATAATTCGTCACCTATCTACAAGCTTTTTGTATAGTTTCATCCATGCCATGTGTAATCCC, followed by the GFP *att*B2-containing primer with GGGGACAACCTTTGTATAATAAAGTT

GCGGTACCTTATAATTCGTCACCTATCTACAAGCTTTTTG (*att*B3 underlined). eYFP was amplified using the primers GGGGA CAGCTTTCTTGACAAAGTGGCACCTAGGGTGAGCAAG GGCGAGGAGCTGTTC (*att*B2 underlined) and GGGGA CCACTTTGTACAAGAAAGCTGGGTCCTGCAGTTACTTTGT ACAGCTCGTCCATGCCGAGA (*att*B3 underlined) from the *T. gondii* vector pTub-eYFP as a template (a kind gift from M. Crawford, University Pennsylvania). DsRED (monomeric version; Campbell *et al.*, 2002) was amplified using the primers GGGGACAGCTTTCTTGACAAAGTGGCACCTAGGAT GGCCTCCTCCGAGGACGTCATCAAGGAGTTCATGC (*att*B2 underlined) and GGGGACAACCTTTGTATAATAAAGTTGCTT AAAGCTTGGCGCCGGTGGAGTGGCGGCCCTCGGCGC GCTCG (*att*B3 underlined) with the *T. gondii* vector P30-mRFP-SDEL-pTub as a template (a kind gift from M. Nishi, University Pennsylvania). The primers were designed to contain the appropriate *att* sites to enable recombination via a BP clonase reaction into the commercially available pDONRP2/P3R vector (Invitrogen). Resulting plasmids were named GFP-pENTR2/3, GFP-SDEL-pENTR2/3, eYFP-pENTR2/3 and DsRED-pENTR2/3 (Fig. 1).

Genes-of-interest were cloned into the commercially available pENTR-D/TOPO vector (Invitrogen), using a topoisomerase I-based reaction. Genes were amplified with the 5' primer containing the CACC motif to facilitate directional cloning using the topoisomerase enzyme. We also included eight base pairs of native sequence upstream of the start codon to avoid problems in translation initiation that may arise from placing an *att* site between the promoter and start codon in the resulting expression vector. The citrate synthase leader [CS(l)] was amplified using the primers CACCTTTAAAAAATGGAAGGAATAAGATACCTATCATGC and TTCAAAAAATTCATAATAACAGATTCTTC, the acyl carrier protein leader [ACP(l)] was amplified using the primers CACCTTATTAGAATGAAGATCTTATTACTTTG and TTTTAAAGAGCTAGATGGG, and the BiP signal peptide [BiP(s)] using the primers CACCATTCAAAAATGAAACAAATTAGG and GTTTGAGTCAACGGCACTTATAAA. The resulting PCR products were mixed as per manufacturer's instructions with pENTR-D/TOPO (Invitrogen) to yield CS(l)-pENTR1/2, ACP(l)-pENTR1/2 and BiP(s)-pENTR1/2 (Fig. 1).

Expression vectors were created with a LR reaction by mixing one of each of the four plasmids in the presence of a recombination enzyme mix following the manufacturer's instructions (Invitrogen). Each reaction consisted of a promoter ENTR clone, one gene ENTR clone and one fluorescent protein ENTR clone together with either pCHDR-3/4 or pHBR-3/4 (Fig. 1). The resultant plasmid contained the gene-of-interest flanked by the promoter and fluorescent protein of choice in a destination (transfection) clone containing the desired selectable marker (Fig. 1B).

### Parasite transfection

Transfections of these plasmids into *P. falciparum* were performed as previously described (Wu *et al.*, 1995; Crabb and Cowman, 1996; Tonkin *et al.*, 2004), and yielded drug-resistant, fluorescent parasites in 15–25 days (slightly longer for the double transfectants), which is rapid and likely due to both a head-to-tail orientation of the expression cassettes and the presence of a rep20 telomere-clustering element. The

D10 strain of *P. falciparum* was used for all transfections except the BiP-GFP-SDEL line, which was transfected into 3D7 parasites. Drug-resistant parasites were selected on either 5 nM WR99210 or 2.5 µg ml<sup>-1</sup> blasticidin S. After stable lines of drug-resistant parasites were obtained, we found that increasing the blasticidin S concentration to 7.5 µg ml<sup>-1</sup> resulted in higher fluorescence levels, presumably because this forced the parasite to maintain more episomal copies of BSD-containing vectors (Mamoun *et al.*, 1999).

Double transgenic parasites were either made by transfecting two separate plasmids at the same time or by sequentially transfecting and selecting for stable parasites with both drugs. Sequential transfection was carried out by transfecting the PfCRT 5'-CS(l)-DsRED-pHBIR-3/4 plasmid on top of already established PfHSP865'-ACP(l)-GFP-pCHDR-3/4 containing parasites. Co-transfection of 100 µg of each plasmid was used to produce the PfHSP865'-CS(l)-YFP-pCHDR-3/4/HSP865'-PfACP(l)-DsRed-pHBI-3/4 containing cell line.

#### Microscopy and immunofluorescence assays

Live parasitized erythrocytes were visualized using Leica confocal microscopes. Rotations were performed using Leica confocal software, and rotation movies created using iMovie 4 (Apple Software). Nuclei were labelled using Hoechst 33258 by incubating live cells for 20 min at a concentration of 20 µg ml<sup>-1</sup>. The life stages of the cells we observed were defined as follows: ring-stage cells were considered to be cells containing a single nucleus and lacking a food vacuole, trophozoite cells were those containing a single nucleus and a pigmented food vacuole, and schizont cells were those containing a pigmented food vacuole and two or more nuclei. IFA were performed following the previously described protocol (Tonkin *et al.*, 2004). *P. falciparum* anti-BiP antibody was obtained through the Malaria Research and Reference Resource Center, NIH (MRA-20, contributed by John Adams; Kumar *et al.*, 1991), and used at a concentration of 1 in 1000. We used Alexa Fluor 594 goat anti-rabbit secondary antibody (Molecular Probes) at a concentration of 1 in 1000.

#### Western blot analysis

Protein samples for Western blot analysis were prepared as previously described (Waller *et al.*, 2000) and membranes probed with mouse anti-GFP (1:2000; Roche) for the BiP(s)-GFP-SDEL Western blot, rabbit anti-GFP (1:5000; Clontech) for the CS(l)-YFP Western blot, and rabbit anti-DsRED (1:5000; a kind gift from Emanuela Handman, Walter and Eliza Hall Institute) for the ACP(l)-DsRED Western. Primary antibody binding was detected using a goat anti-mouse or goat anti-rabbit antibody conjugated to horseradish peroxidase (Pierce).

#### Acknowledgements

We are grateful to T. Voss, M. Crawford and M. Nishi for supplying vectors, E. Handman for providing anti-DsRed antibody and T. Spurck for assistance with confocal microscopy. GvD is supported by an Australian Postgraduate Award and CJT by a Melbourne Research Scholarship. This work was

supported by the NHMRC and the Wellcome Trust. M.M. is supported by a postdoctoral fellowship from the Swiss National Science Foundation, G.I.M. and A.F.C. are supported by HHMI International Research Scholar Grants. G.I.M. also gratefully acknowledges an ARC Professorial Fellowship.

#### References

- Adisa, A., Rug, M., Klonis, N., Foley, M., Cowman, A.F., and Tilley, L. (2003) The signal sequence of exported protein-1 directs the green fluorescent protein to the parasitophorous vacuole of transfected malaria parasites. *J Biol Chem* **278**: 6532–6542.
- Aikawa, M. (1966) The fine structure of the erythrocytic stages of three avian malarial parasites, *Plasmodium falciparum*, *P. lophurae*, and *P. cathemerium*. *Am J Trop Med Hyg* **15**: 449–471.
- Aikawa, M., Hepler, P.K., Huff, C.G., and Sprinz, H. (1966) The feeding mechanism of avian malarial parasites. *J Cell Biol* **28**: 355–373.
- Allewa, L.M., and Kirk, K. (2001) Calcium regulation in the intraerythrocytic malaria parasite *Plasmodium falciparum*. *Mol Biochem Parasitol* **117**: 121–128.
- Andres, D.A., Dickerson, I.M., and Dixon, J.E. (1990) Variants of the carboxyl-terminal KDEL sequence direct intracellular retention. *J Biol Chem* **265**: 5952–5955.
- Arimura, S., Yamamoto, J., Aida, G.P., Nakazono, M., and Tsutsumi, N. (2004) Frequent fusion and fission of plant mitochondria with unequal nucleoid distribution. *Proc Natl Acad Sci USA* **101**: 7805–7808.
- Bannister, L.H., Hopkins, J.M., Fowler, R.E., Krishna, S., and Mitchell, G.H. (2000) A brief illustrated guide to the ultrastructure of *Plasmodium falciparum* asexual blood stages. *Parasitol Today* **16**: 427–433.
- Baunaure, F., Eldin, P., Cathiard, A.M., and Vial, H. (2004) Characterization of a non-mitochondrial type I phosphatidylserine decarboxylase in *Plasmodium falciparum*. *Mol Microbiol* **51**: 33–46.
- Bozdech, Z., Llinas, M., Pulliam, B.L., Wong, E.D., Zhu, J., and DeRisi, J.L. (2003) The transcriptome of the intraerythrocytic developmental cycle of *Plasmodium falciparum*. *PLoS Biol* **1**: E5.
- Campbell, R.E., Tour, O., Palmer, A.E., Steinbach, P.A., Baird, G.S., Zacharias, D.A., and Tsien, R.Y. (2002) A monomeric red fluorescent protein. *Proc Natl Acad Sci USA* **99**: 7877–7882.
- Couffin, S., Hernandez-Rivas, R., Blisnick, T., and Mattei, D. (1998) Characterisation of PfSec61, a *Plasmodium falciparum* homologue of a component of the translocation machinery at the endoplasmic reticulum membrane of eukaryotic cells. *Mol Biochem Parasitol* **92**: 89–98.
- Cowman, A.F., and Crabb, B.S. (2002) The *Plasmodium falciparum* genome – a blueprint for erythrocyte invasion. *Science* **298**: 126–128.
- Crabb, B.S., and Cowman, A.F. (1996) Characterization of promoters and stable transfection by homologous and non-homologous recombination in *Plasmodium falciparum*. *Proc Natl Acad Sci USA* **93**: 7289–7294.
- Crabb, B.S., Triglia, T., Waterkeyn, J.G., and Cowman, A.F.



- (1997) Stable transgene expression in *Plasmodium falciparum*. *Mol Biochem Parasitol* **90**: 131–144.
- Delorenzi, M., Sexton, A., Shams-Eldin, H., Schwarz, R.T., Speed, T., and Schofield, L. (2002) Genes for glycosylphosphatidylinositol toxin biosynthesis in *Plasmodium falciparum*. *Infect Immun* **70**: 4510–4522.
- Divo, A.A., Geary, T.G., Jensen, J.B., and Ginsburg, H. (1985) The mitochondrion of *Plasmodium falciparum* visualized by rhodamine 123 fluorescence. *J Protozool* **32**: 442–446.
- Eckstein-Ludwig, U., Webb, R.J., Van Goethem, I.D., East, J.M., Lee, A.G., Kimura, M., et al. (2003) Artemisinins target the SERCA of *Plasmodium falciparum*. *Nature* **424**: 957–961.
- Elmendorf, H.G., and Haldar, K. (1993) Identification and localization of ERD2 in the malaria parasite *Plasmodium falciparum*: separation from sites of sphingomyelin synthesis and implications for organization of the Golgi. *EMBO J* **12**: 4763–4773.
- Fidock, D.A., and Wellems, T.E. (1997) Transformation with human dihydrofolate reductase renders malaria parasites insensitive to WR99210 but does not affect the intrinsic activity of proguanil. *Proc Natl Acad Sci USA* **94**: 10931–10936.
- Foth, B.J., Ralph, S.A., Tonkin, C.J., Struck, N.S., Fraunholz, M., Roos, D.S., et al. (2003) Dissecting apicoplast targeting in the malaria parasite *Plasmodium falciparum*. *Science* **299**: 705–708.
- Francis, S.E., Sullivan, D.J., Jr, and Goldberg, D.E. (1997) Hemoglobin metabolism in the malaria parasite *Plasmodium falciparum*. *Annu Rev Microbiol* **51**: 97–123.
- Hopkins, J., Fowler, R., Krishna, S., Wilson, I., Mitchell, G., and Bannister, L. (1999) The plastid in *Plasmodium falciparum* asexual blood stages: a three-dimensional ultrastructural analysis. *Protist* **150**: 283–295.
- Jomaa, H., Wiesner, J., Sanderbrand, S., Altincicek, B., Weidemeyer, C., Hintz, M., et al. (1999) Inhibitors of the non-mevalonate pathway of isoprenoid biosynthesis as antimalarial drugs. *Science* **285**: 1573–1576.
- Jouhet, J., Marechal, E., Baldan, B., Bligny, R., Joyard, J., and Block, M.A. (2004) Phosphate deprivation induces transfer of DGDG galactolipid from chloroplast to mitochondria. *J Cell Biol* **167**: 863–874.
- Kadekoppala, M., Cheresch, P., Catron, D., Ji, D.D., Deitsch, K., Wellems, T.E., et al. (2001) Rapid recombination among transfected plasmids, chimeric episome formation and trans gene expression in *Plasmodium falciparum*. *Mol Biochem Parasitol* **112**: 211–218.
- Klemba, M., Beatty, W., Gluzman, I., and Goldberg, D.E. (2004) Trafficking of plasmepsin II to the food vacuole of the malaria parasite *Plasmodium falciparum*. *J Cell Biol* **164**: 47–56.
- Kumar, N., Koski, G., Harada, M., Aikawa, M., and Zheng, H. (1991) Induction and localization of *Plasmodium falciparum* stress proteins related to the heat shock protein 70 family. *Mol Biochem Parasitol* **48**: 47–58.
- La Greca, N., Hibbs, A.R., Riffkin, C., Foley, M., and Tilley, L. (1997) Identification of an endoplasmic reticulum-resident calcium-binding protein with multiple EF-hand motifs in asexual stages of *Plasmodium falciparum*. *Mol Biochem Parasitol* **89**: 283–293.
- McFadden, G.I., Reith, M.E., Munholland, J., and Lang-Unnasch, N. (1996) Plastid in human parasites. *Nature* **381**: 482.
- McMillan, P.J., Stimmler, L.M., Foth, B.J., McFadden, G.I., and Müller, S. (2004) The human malaria parasite *Plasmodium falciparum* possesses two distinct dihydrolipoamide dehydrogenases. *Mol Microbiol* **55**: 27–38.
- Mamoun, C.B., Gluzman, I.Y., Goyard, S., Beverley, S.M., and Goldberg, D.E. (1999) A set of independent selectable markers for transfection of the human malaria parasite *Plasmodium falciparum*. *Proc Natl Acad Sci USA* **96**: 8716–8720.
- Marti, M., Good, R.T., Rug, M., Knuepfer, E., and Cowman, A.F. (2004) Targeting malaria virulence and remodeling proteins to the host erythrocyte. *Science* **306**: 1930–1933.
- Meeusen, S., McCaffery, J.M., and Nunnari, J. (2004) Mitochondrial fusion intermediates revealed *in vitro*. *Science* **305**: 1747–1752.
- Morrisette, N.S., and Sibley, L.D. (2002) Cytoskeleton of apicomplexan parasites. *Microbiol Mol Biol Rev* **66**: 21–38.
- Munro, S., and Pelham, H.R. (1987) A C-terminal signal prevents secretion of luminal ER proteins. *Cell* **48**: 899–907.
- O'Donnell, R.A., Freitas-Junior, L.H., Preiser, P.R., Williamson, D.H., Duraisingh, M., McElwain, T.F., et al. (2002) A genetic screen for improved plasmid segregation reveals a role for Rep20 in the interaction of *Plasmodium falciparum* chromosomes. *EMBO J* **21**: 1231–1239.
- Ralph, S.A., Van Dooren, G.G., Waller, R.F., Crawford, M.J., Fraunholz, M.J., Foth, B.J., et al. (2004) Tropical infectious diseases: metabolic maps and functions of the *Plasmodium falciparum* apicoplast. *Nat Rev Microbiol* **2**: 203–216.
- Santiago, T.C., Zufferey, R., Mehra, R.S., Coleman, R.A., and Mamoun, C.B. (2004) The *Plasmodium falciparum* PfGatp is an endoplasmic reticulum membrane protein important for the initial step of malarial glycerolipid synthesis. *J Biol Chem* **279**: 9222–9232.
- Sato, S., Rangachari, K., and Wilson, R.J. (2003) Targeting GFP to the malarial mitochondrion. *Mol Biochem Parasitol* **130**: 155–158.
- Sato, S., Clough, B., Coates, L., and Wilson, R.J. (2004) Enzymes for heme biosynthesis are found in both the mitochondrion and plastid of the malaria parasite *Plasmodium falciparum*. *Protist* **155**: 117–125.
- Semenza, J.C., Hardwick, K.G., Dean, N., and Pelham, H.R. (1990) ERD2, a yeast gene required for the receptor-mediated retrieval of luminal ER proteins from the secretory pathway. *Cell* **61**: 1349–1357.
- Slomianny, C., and Prensier, G. (1986) Application of the serial sectioning and tridimensional reconstruction techniques to the morphological study of the *Plasmodium falciparum* mitochondrion. *J Parasitol* **72**: 595–598.
- Soldati, D., and Meissner, M. (2004) *Toxoplasma* as a novel system for motility. *Curr Opin Cell Biol* **16**: 32–40.
- Srivastava, I.K., Morrissey, J.M., Darrouzet, E., Daldal, F., and Vaidya, A.B. (1999) Resistance mutations reveal the atovaquone-binding domain of cytochrome b in malaria parasites. *Mol Microbiol* **33**: 704–711.
- Striepen, B., Crawford, M.J., Shaw, M.K., Tilney, L.G., Seeber, F., and Roos, D.S. (2000) The plastid of *Toxoplasma*

- gondii* is divided by association with the centrosomes. *J Cell Biol* **151**: 1423–1434.
- Surolia, N., and Surolia, A. (2001) Triclosan offers protection against blood stages of malaria by inhibiting enoyl-ACP reductase of *Plasmodium falciparum*. *Nat Med* **7**: 167–173.
- Tonkin, C.J., van Dooren, G.G., Spurck, T.P., Struck, N.S., Good, R., Handman, E., *et al.* (2004) Localization of organellar proteins in *Plasmodium falciparum* using a novel set of transfection vectors and a new immunofluorescence fixation method. *Mol Biochem Parasitol* **137**: 13–21.
- van Dooren, G.G., Su, V., D'Ombrain, M.C., and McFadden, G.I. (2002) Processing of an apicoplast leader sequence in *Plasmodium falciparum* and the identification of a putative leader cleavage enzyme. *J Biol Chem* **277**: 23612–23619.
- Van Wye, J., Ghori, N., Webster, P., Mitschler, R.R., Elmen-dorf, H.G., and Haldar, K. (1996) Identification and localization of rab6, separation of rab6 from ERD2 and implications for an 'unstacked' Golgi, in *Plasmodium falciparum*. *Mol Biochem Parasitol* **83**: 107–120.
- Varadharajan, S., Dhanasekaran, S., Bonday, Z.Q., Ranga-rajana, P.N., and Padmanaban, G. (2002) Involvement of delta-aminolaevulinate synthase encoded by the parasite gene in de novo haem synthesis by *Plasmodium falciparum*. *Biochem J* **367**: 321–327.
- Voelker, D.R. (2004) Genetic analysis of intracellular aminoglycerophospholipid traffic. *Biochem Cell Biol* **82**: 156–169.
- Waller, R.F., and McFadden, G.I. (2005) The apicoplast: a review of the derived plastid of apicomplexan parasites. *Curr Issues Mol Biol* **7**: 57–79.
- Waller, R.F., Keeling, P.J., Donald, R.G.K., Striepen, B., Handman, E., Lang-Unnasch, N., *et al.* (1998) Nuclear-encoded proteins target to the plastid in *Toxoplasma gondii* and *Plasmodium falciparum*. *Proc Natl Acad Sci USA* **95**: 12352–12357.
- Waller, R.F., Reed, M.B., Cowman, A.F., and McFadden, G.I. (2000) Protein trafficking to the plastid of *Plasmodium falciparum* is via the secretory pathway. *EMBO J* **19**: 1794–1802.
- Waller, R.F., Ralph, S.A., Reed, M.B., Su, V., Douglas, J.D., Minnikin, D.E., *et al.* (2003) A type II pathway for fatty acid biosynthesis presents drug targets in *Plasmodium falciparum*. *Antimicrob Agents Chemother* **47**: 297–301.
- Wickham, M.E., Rug, M., Ralph, S.A., Klonis, N., McFadden, G.I., Tilley, L., and Cowman, A.F. (2001) Trafficking and assembly of the cytoadherence complex in *Plasmodium falciparum*-infected human erythrocytes. *EMBO J* **20**: 5636–5649.
- Wu, Y., Sifri, C.D., Lei, H.H., Su, X.Z., and Wellems, T.E. (1995) Transfection of *Plasmodium falciparum* within human red blood cells. *Proc Natl Acad Sci USA* **92**: 973–977.

### Supplementary material

The following supplementary material is available for this article online:

**Fig. S1.** Sequential transfection of *P. falciparum* with ACP(I)-GFP and CS(I)-DsRed using two selectable markers.

**Movies S1–S8.** Rotation movies of ACP(I)-DsRed and CS(I)-YFP double transfectant parasites.